

CFD – BASED STUDY ON GOLDSCHMIED PROPULSION CONCEPT APPLICATION FOR DRAG REDUCTION

Cecil W. Skaleski*, Felipe I. K. Odaguil†, Joao H. A. Azevedo†, Leandro S. M. Lima†,
Roberto A. S. Cardoso†, Paulo H. Iscold‡

*Instituto Tecnológico de Aeronáutica

†Embraer

‡Universidade Federal de Minas Gerais

Keywords: *Drag reduction, CFD, DOE, pressure thrust, propulsive integration*

Abstract

The propulsive concept of Goldschmied-Skaleski proposes simultaneously the drag reduction of an aerodynamic body and the increase of propulsive efficiency through the ingestion and control of the boundary layer. In an effort to increase the technology readiness level of this concept, the authors apply it to the aerodynamic design of a main landing gear wheel fairing of a racer aircraft named Anequim designed to be the fastest piston engine aircraft in the world. Over this test model, a design of experiments methodology was used with almost 2,700 different geometries to study the influence of specific design parameters over the overall drag force. This study was carried out using 2-D and 3-D CFD simulations provided by commercial software. The relevant design parameters were identified using a correlation matrix of the 2-D results. Finally, in order to verify the proposed methodology a 3-D CFD simulation was performed. The results show a reduction on the drag force of the wheel fairing for an operational range of the suction system and also an increase on the axial force due to the fan thrust.

1. Introduction

1.1. Motivation and Objective

The propulsive concept of Goldschmied-Skaleski has shown to be a promising technology in the sense of drag reduction as demonstrated in previous studies by Skaleski

[1]. In order to increase the technology readiness level of this concept, a cooperative workgroup was formed by academia professors, students and industry professionals to study and apply this concept to a lightweight speed competition aircraft.

To better assess the effectiveness of this concept and to measure the potential gains attained through this technology, it was tested on a single component of the aircraft: the main landing gear wheel fairing. The complete work was initially divided into three stages: the aerodynamic design of this component, its wind tunnel testing and a final flight test.

The present paper describes the first part of this effort; the aerodynamic design of the wheel fairing of an airplane named Anequim. The goal of this aircraft, which is being developed by the Center for Aeronautical Studies of the Federal University of Minas Gerais (UFMG-CEA), is to become the fastest aircraft in its class. Thus, the authors' main objective is to reduce the total drag of the component/aircraft through the implementation of the present propulsive concept.

1.2. The Propulsive Concept of Goldschmied-Skaleski

The propulsive concept of Goldschmied-Skaleski, first developed 1954 [2] and further improved in 2014 [1], consists in the control of a body's boundary layer through a propulsive system. The application of this concept has already shown [1] to allow for a 64% drag

reduction over an axisymmetric body, which confirms the initial study by Goldschmied [2].

Goldschmied's original concept, see Figure 1, uses a powertrain to apply suction to the boundary layer, thereby avoiding its detachment. This also increased the propulsive efficiency of the system since the ingested boundary layer air has less momentum than the freestream air flow.



Figure 1—Original propulsive concept.

For 60 years this concept remained doubtful since no experiment was made to reproduce the original observations. In 2012, Roepke [3], Seubert [4] and Thomason [5] performed wind tunnel testing and CFD simulations that allowed Skaleski [1] to enhance the original concept. By adding an aerodynamic component in powertrain installation, the later author was able to reduce the total drag of the system.

1.3. Anequim

The CEA-UFMG holds four world records with CEA-308 aircraft (FAI Category C-1.a0 - 0 to 300 kg MTOW):

- 1) Time to Climb to 3,000 Meters: 8 min 15 s;
- 2) Speed Over 15 km Course: 329.1 km/h;
- 3) Speed Over a Closed Course 100 km: 326.8 km/h;
- 4) Speed Over a 3 km Course: 360.13 km/h.

The Anequim, as seen in Figure 2, is a single-seat aircraft, equipped with a 4 cylinder engine and weighs less than 500 kg (Category FAI C-1.a – 300 to 500 kg MTOW). The working group intends to reach a top speed of 575 kph (310 kts) with this aircraft. This result

would grant the Anequim the title of fastest aircraft equipped with a piston engine.

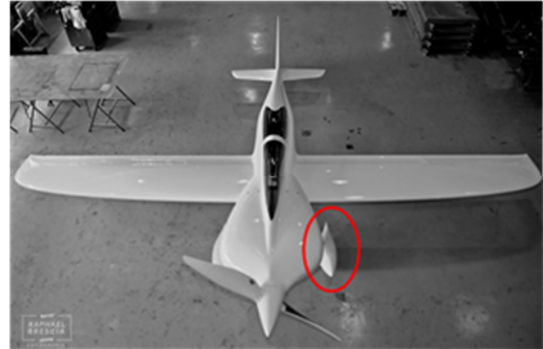


Figure 2 – Anequim and the wheel fairing.

This is a study which is separated from the aircraft design itself and aims solely to contribute to its drag reduction. Thus, although the aircraft is used as a test platform for the development of this technology, the airplane flight schedules are unaffected by the present development.

Moreover, in order to reduce weight and simplify the landing gear system, the aforementioned aircraft is equipped with a fixed undercarriage. Despite their constructive advantages the fixed landing gear contributes a considerable amount to total drag of the aircraft [6]. The landing gear fairings involve the wheels and are designed to reduce the form drag due to the wheel. Nevertheless, due to its large contribution to the total drag of the airplane, the fairings from the main landing gear of the Anequim were chosen as the starting point for the application of this technology.

The results later discussed in this work show that the drag caused by the landing gear fairing was reduced substantially; therefore allowing the aircraft speed to be increased.

An Electric Ducted Fan (EDF) propulsive system is essentially a propeller driven by an electric motor enveloped by a duct or fairing. Due to design requirements, which will be discussed later, the EDF system that came closest to the desired performance was the Schubeler DS-51-DIA HDT, which has the characteristics described in Table 1.

Table 1 – EDF system main characteristics.

Diameter [m]	Max Static Thrust [N]	Exhaust Speed [m/s]	Power [kW]
0.09	33	85	1.9

According to previous studies by Skaleski [1], it is necessary that the fan exhaust speed be greater than the free stream air speed in order to observe the effects of drag reduction. As a result the design point of the new wheel fairing was set to 75 m/s, which also allows the concept to be evaluated in the available wind tunnel.

2. Proposed Methodology

2.1. Design Requirements

Some requirements were imposed directly and other restrictions arose indirectly. The direct requirements are:

- 1) The geometries of the original and modified fairing should be interchangeable, allowing the assembly of two geometries in the plane quickly and easily and disassembling the minimum number of components from the original main landing gear;
- 2) The fan motor must be electric in order to harness the energy from the engine starting battery installed within the aircraft;
- 3) The fan assembly should be commercially available (off the shelf);
- 4) The air flow speed exiting the fan should be compatible with the aircraft flight speed.

Among the indirect requirements are: the minimum thickness of the airfoil trailing edge used in the shroud, the fan diameter and overall ease of assembly.

2.2. Physical Modeling and Solution Strategy

The model problem being considered in the present work consists of a teardrop-like body subjected to a subsonic flow at a low Reynolds number condition. Although this might lead one to consider modeling this scenario as a low-speed aerodynamics problem, the application of the propulsive concept might lead certain regions of the flow to reach higher Mach numbers, *i.e.*, reach sonic conditions.

Hence, to better represent the physics of these conditions, the flow was modeled through the compressible RANS equations with a shear stress transport turbulence modeling. Moreover, the authors have chosen to use the commercial

solver CFD++ [7] to perform the aerodynamic calculations required.

Naturally, this choice impacts the geometric modeling and meshing schemes which will be discussed later in the paper. For the moment, it suffices to explain that the 2-D solutions provided by the solver will be used to drive a design of experiments process that seeks to optimize certain design parameters. The improved 2-D geometry is, then, expanded back to a 3-D model so that the improvements from this concept can be better assessed. The drag force was nondimensionalized according to

$$C_D = \frac{D}{\frac{1}{2}\rho_\infty U_\infty^2 S_{ref}}, \quad (1)$$

where C_D is the drag coefficient and S_{ref} is the wheel fairing maximum cross section area for the 3-D case.

The equivalent diameter was calculated using this area value then used to nondimensionalize the 2-D data. The resulting force in x axis direction coefficient and the fan thrust coefficient were obtained respectively by

$$C_x = \frac{F_x}{\frac{1}{2}\rho_\infty U_\infty^2 S_{ref}} \quad (2)$$

and

$$C_T = \frac{T}{\frac{1}{2}\rho_\infty U_\infty^2 S_{ref}}. \quad (3)$$

The suction coefficient is defined by

$$C_q = \frac{\dot{m}_{fan}}{\rho_\infty U_\infty S_{ref}}, \quad (4)$$

where \dot{m}_{fan} is the air mass flow passing through the fan and the fan power coefficient is calculated as

$$C_{pw} = \frac{C_q \Delta P_{T,fan}}{\rho_\infty}, \quad (5)$$

where $\Delta P_{T,fan}$ is the mean total pressure difference between the fan air inlet and outlet.

2.3. Geometric Model

Due to the design constraints, the fairing was split into front and rear parts as shown in Figure 3. The front part carries the tire, brake assembly and the anchor leg of the landing gear. This part will not be changed in order to meet the first requirement set forth previously.

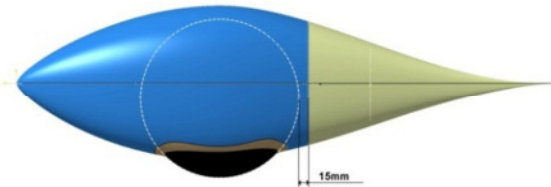


Figure 3 – Wheel fairing division.

To design the rear section of the fairing, the authors used a cutting plane positioned 15 mm after the circumference of the tire. The preliminary aerodynamic design was based on the initial study by Skaleski [1] according to which the fan should be positioned as far as possible from the front section. An initial assessment showed that a 90 mm diameter fan would meet requirements 3 and 4, being positioned as far away from the front section as possible. A NACA 4-digit generic airfoil is used to generate the preliminary shroud geometry, resulting in a revolution surface with constant section as shown in Figure 4.

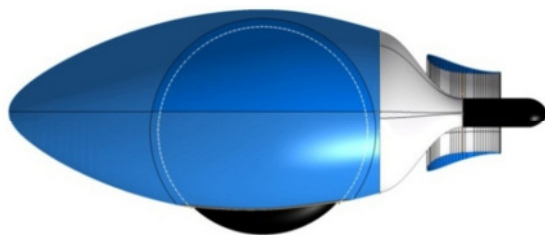


Figure 4 – Sliced view of preliminary design.

From the preliminary geometry two 2-D sketches were extracted from the intersection of the 3-D model with two longitudinal cutting planes. These planes have been positioned such that the 2-D geometries represent critical sections of the initial 3-D geometry. Figure 5 illustrates this procedure.

The 2-D model had its defining curves parameterized directly in CATIA [8]. Thus, by varying such parameters, it was possible to generate any NACA 4-digits airfoil with only

two curves: one for the upper and one for the lower side of the airfoil. This parameterization was also restricted to meet the construction design requirements. Figure 6 and Figure 7 illustrate some of the shapes generated in each cut.

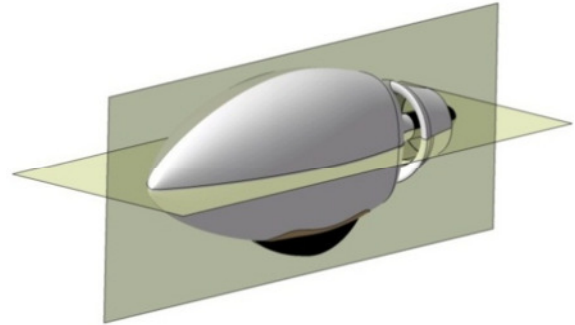


Figure 5 – Perpendicular cut planes.

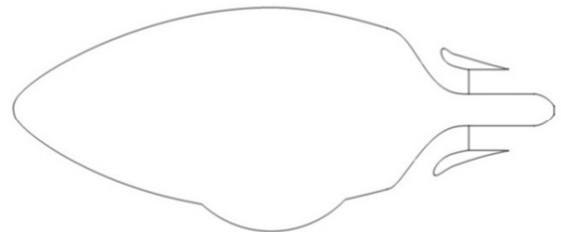


Figure 6 – Wheel side cut plane.

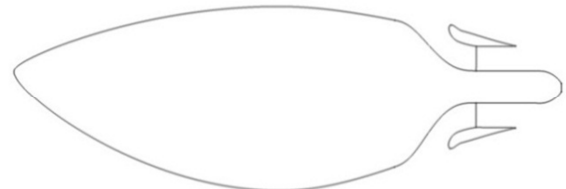


Figure 7 – Smooth side cut plane.

Thus, it was possible to obtain complex geometries ranging five parameters at each side of the geometry. Since the 2-D models have their parameters defined based on the results of CFD simulations, it was necessary to reconstruct the 3-D model using the same parameters. To accomplish this, the authors used a multi-section lofting with surface tangency, which allows the generation of an interpolated surface between each modified cut section.

2.4. Mesh Generation

The two-dimensional meshes are constructed so as to allow their generation over similar geometries to be automated, given that a

large number of simulations would be required. The meshing scheme adopted in the present work uses structured hexahedral meshes generated by ICEM [9].

A C-grid strategy was used for the construction of the 2-D blocking in order to fit the geometry of the fairing and shroud. The blocking is composed of 3 layers: the first and third one serves to refine the mesh at the boundary layer region of the entire fairing and the second layer contains the blocks that were removed to generate the shroud. Control points were created to position the vertices of each block in pre-determined locations which are automatically created from the fairing surface. This allowed the authors to create very similar meshes for a large number of similar geometries.

The mesh spacing is controlled with bi-exponential laws and the thickness of the first element, adjacent to the model surface, is fixed in order to keep y^+ equal to 30. The final 2-D meshes have around 86,000 elements, as seen in Figure 8 and Figure 9.

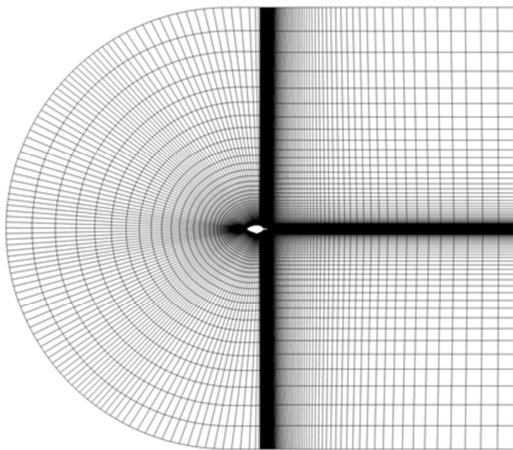


Figure 8 – Complete 2-D structured mesh.

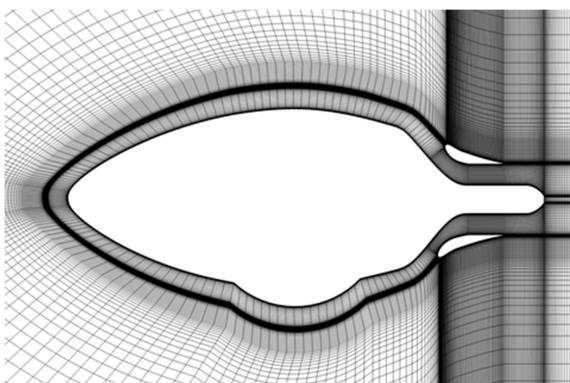


Figure 9 – Close-up of mesh near the wheel fairing.

Although the process was illustrated with the vertical cut plane, the same mesh blocking and bunching parameters were used for the meshes of the horizontal cut plane and the meshes of the original fairing without the suction system.

The same concept of blocking layers used in the 2-D grids was expanded to the 3-D models. The final 3-D mesh has 5 million volumetric elements and 200,000 surface elements as shown in Figure 10 and Figure 11.

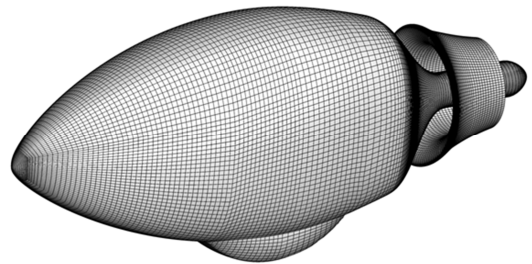


Figure 10 – 3-D structured mesh on proposed fairing.

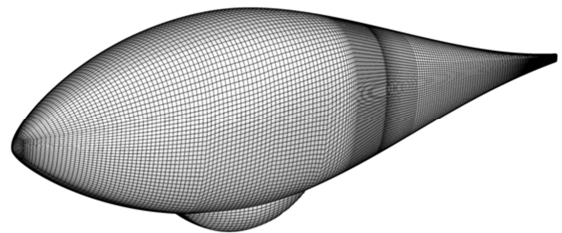


Figure 11 – 3-D structured mesh on original fairing.

Finally, the far field boundaries for all of the generated meshes were set at twenty five wheel fairing lengths away from the model.

2.5. Boundary and Simulation Conditions

The computational model consists of three boundaries: a non-slip adiabatic wall, a farfield where the freestream conditions are imposed and a flow through with static pressure jump (ΔP_s) in order to model the fan. The values imposed in the two later boundaries are described in Table 2. Moreover, the value adopted for ΔP_s is the dynamic pressure required to accelerate the air from zero to 85 m/s; which is assumed as a desired outflow velocity for the fan according to the studies of Skaleski [1].

Table 2 – 2-D simulation conditions.

Mach No.	ρ [kg/m ³]	Reynolds No.	ΔP_s [Pa]
0.22	1.225	$3.59 \cdot 10^6$	4,425

For 3-D analysis, cases with different pressure jumps on the fan boundary, other than indicated in Table 2, were evaluated in order to assess the variation of the resultant force with the jump in pressure at the fan. The values for ΔP_s in these cases ranged from zero to 20,000 Pa. Aside from the pressure jump, the other flight conditions for the 3-D simulations were the same as the 2-D conditions previously established.

2.6. Design of Experiments

In order to fully exploit the design space for each of the analyzed airfoils, a full factorial design of experiments was created. The full factorial design of experiments is a project type where it is possible to study the effects of the interactions between relevant factors given that it covers all possible combinations among each factor involved in the analysis [10]. The main purpose of this procedure is to analyze the influence of each parameter in the fairing design. The minimum and maximum values for each of the variables are defined based on typical values found in similar airfoils. The discretization used in each case is shown in Table 3. For the present study, a total of 675 geometries were generated for each airfoil totaling 2,700 configurations.

Table 3 – design variable discretization.

Variable	Minimum	Maximum	Levels
p	0.20	0.40	3
m	0.07	0.11	5
chord	80	110	5
Tension1	0.40	1.00	3
Tension2	0.40	1.00	3

3. Results

3.1. Correlation Matrix

Four correlation matrices, one for each airfoil, were obtained. These matrices correlate the influence of each input parameter of the geometric model with the measured variables in

the CFD simulations. Figure 12 shows the correlation matrix obtained for the case of the lower airfoil surface in the vertical plane. Although not shown in the present work, the other three matrices presented similar responses.

Each cell below the main diagonal represents the intensity of the correlation of two given parameters. The main diagonal shows the distribution of each parameter in the statistical experiment and scatter plots above the diagonal show the correlation of output variables.

From the correlation matrix, one observes that the resulting variables which influenced the aerodynamic force the most are the chord, Tension 1 and Tension 2. The strong correlation of the aforementioned parameters with the resulting force is due to the fact that, by changing the geometry of the profile and the loft of the air intake, these parameters alter the gap between the surfaces that constitute the system air intake. The gap directly affects the flow of air through the fan (suction coefficient, C_q), which is a parameter that inversely affects the overall force coefficient with a high correlation coefficient of -0.928. The negative sign is due to the resultant force being oriented in the opposite direction of the x axis, which is aligned with the freestream. More to the point, this behavior is due to the fact that, within the Goldschmied-Skaleski proposition, the traction force is a function of air flow through the fan [1]. The m and p parameters, on the other hand, present a low correlation with the size of the gap and, hence, have a low correlation with the resultant force.

It is interesting to note that the force coefficients in the underside airfoil form a cloud of points that assumes a parabolic shape when correlated with the resultant force. This indicates that for the same airfoil aerodynamic force value is possible to obtain two points with different values of overall resulting force. These points have different values of gap and, therefore, a different airflow through the fan. Interestingly, maximizing the aerodynamic force at the airfoils does not lead to a strongest overall resulting force. This is due to the fact that, the greater the aerodynamic force in the airfoil, the greater is the interference field of low pressure created by it on the lofting surface

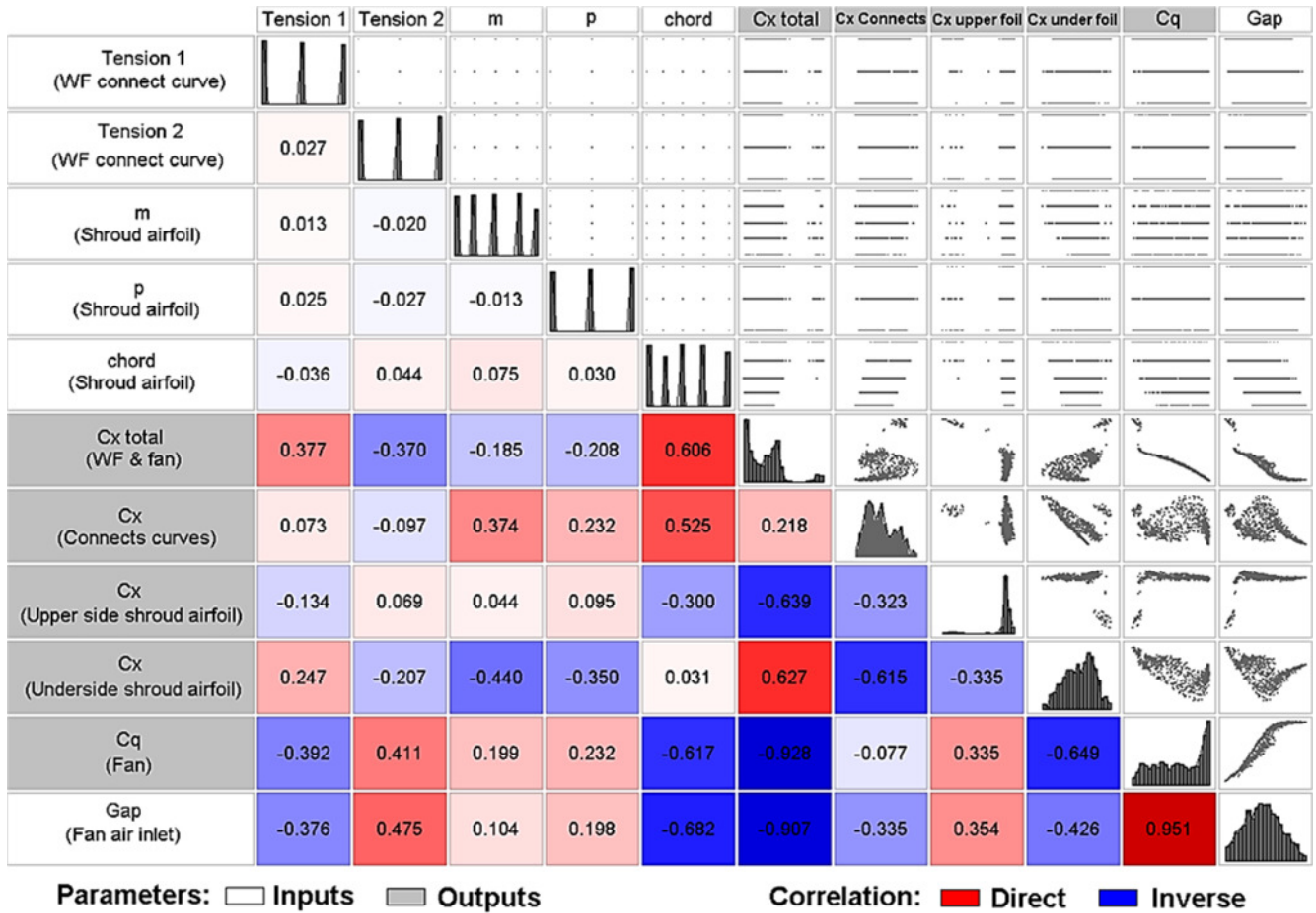


Figure 12 – Correlation matrix for the underside airfoil of the 2-D new wheel fairing results.

that connects to the fan, which increases the overall drag [1]. Therefore, there is a compromise between the aerodynamic force at the profile and the geometry of the lofting surface upstream of the fan.

Finally, one also observes that, from a given value, increasing the gap produces no increase in airflow through the fan, C_q , as indicated in the rightmost column of the second to last line in Figure 12. This highlights the importance of such a preliminary exploratory analysis.

3.2. New Wheel Fairing Results

Figure 13 shows a plot for the total pressure coefficient over the 2-D geometry which the geometric parameter combination showed the highest resultant force. The resultant force is the sum of the reduction in aerodynamic drag and the thrust of the fan. The aforementioned geometry displays good aerodynamic performance with a thin and almost fully attached boundary, even when

considering downstream regions from the tire. Moreover, the mass flow distribution on the fan boundary was nearly uniform, which promotes better fan efficiency.

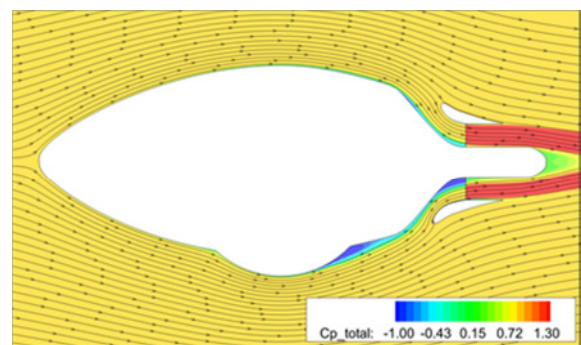


Figure 13 – 2-D total pressure coefficient and streamlines.

The 3-D model of wheel fairing with the suction system was constructed using the parameters from the 2-D results with the highest resultant forces for each case. The Figure 14 shows the total pressure coefficient and

streamlines plotted on the tire section of the 3-D solution.

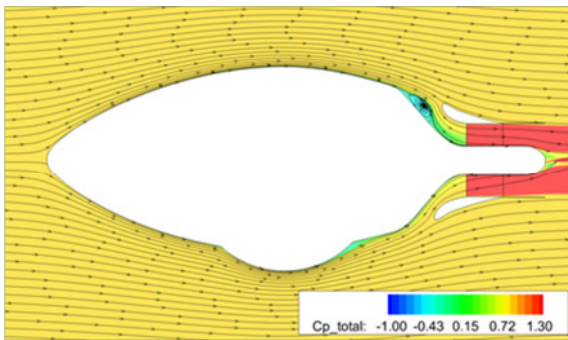


Figure 14 – 3-D total pressure coefficient.

There are some differences the aforementioned results with the previous 2-D equivalent. For instance, it is possible to see a detachment and recirculation region on the upper side air inlet in Figure 14 which did not obstruct the air intake. Also, the downstream regions from the tire show greater attachment on the 3-D case than on the 2-D. Nevertheless, the mass flux through the fan is also uniformly distributed on the boundary.

To better compare the results for the 2-D and 3-D models, one must plot the pressure coefficient distribution over length of the wheel fairing. Figure 15 shows a comparison of the new geometry over the original (clean) wheel fairing. This figure also serves as a placing reference for the pressure coefficient plots that follow.

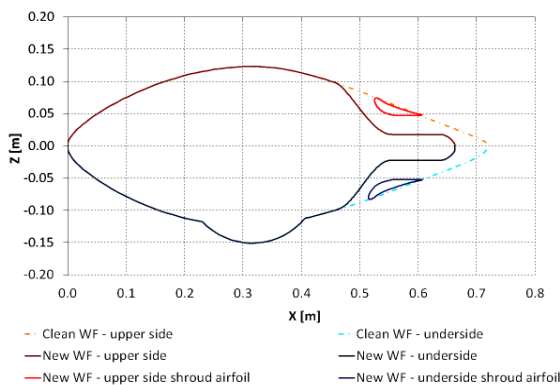


Figure 15 – Tire section geometries plot.

Figure 16 shows the pressure coefficient plot for the original fairing while Figure 17 and Figure 18 show, respectively, the pressure distribution for the main body and shroud airfoils of the new wheel fairing configuration.

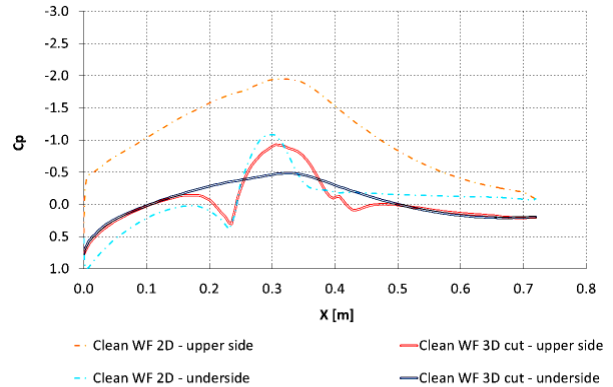


Figure 16 – Clean wheel fairing 2-D and 3-D pressure coefficient distribution.

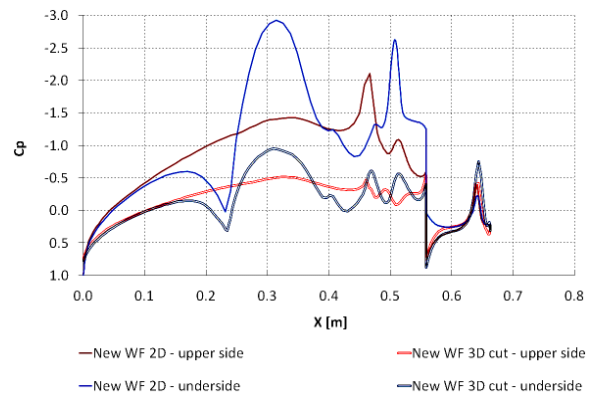


Figure 17 – New wheel fairing pressure coefficient distribution.

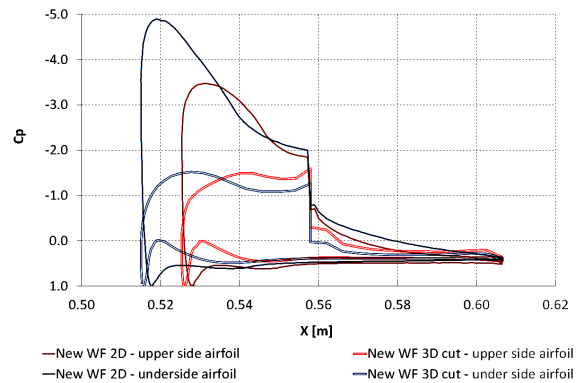


Figure 18 – Shroud airfoils pressure coefficient distribution.

From Figure 16 it is possible to observe that the clean configuration 2-D model achieved a suction peak much higher than the 3-D model, higher aerodynamic loading and lower pressure recovery. The new configuration, on the other hand, achieved greater pressure recovery due to the suction created by the fan and there is a great influence from the shroud airfoil in the wheel fairing, such as the pressure peaks before the fan region shown in Figure 17.

It is interesting to observe in Figure 18 that the stagnation point on the shroud airfoil differs when comparing 2-D to 3-D results; which is due to a difference in the local angle of attack. The 2-D airfoil has greater local angle of attack, so the stagnation point is located further downstream than the 3-D equivalent as shown in Figure 19. Consequently, the aerodynamic loading on the 2-D airfoil is greater than on the 3-D airfoil for similar flow velocities.

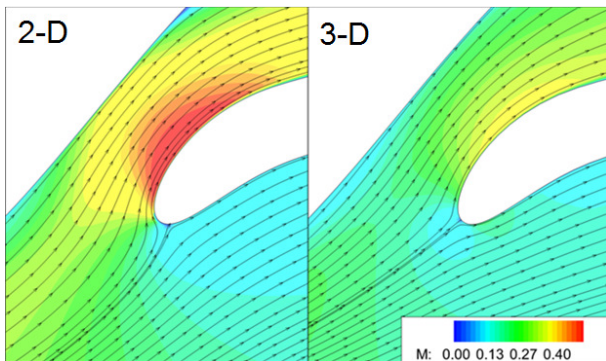


Figure 19 – Stagnation point at 2-D and 3-D cases.

Since the three-dimensional results were nondimensionalized using the maximum cross section area value, the 2-D data is nondimensionalized using the equivalent diameter. The results are shown in Table 4.

Table 4 – 2-D and 3-D results for fan ΔP of 4425Pa.

Case	C_q	C_x	C_t	C_d	C_{pw}
Clean – wheel side	0	0.1731	0	0.1731	0
Clean – Lateral	0	0.0495	0	0.0495	0
Clean – 3-D	0	0.0412	0	0.0412	0
New – Wheel side	0.27	-0.1472	-0.2737	0.1265	926
New – Lateral	0.31	-0.2071	-0.2687	0.0615	1,041
New – 3-D	0.17	-0.1028	-0.4224	0.0464	570

The drag of the 2-D new configuration tire section was reduced by 27% when compared with the same section of the clean configuration, but for the 2-D new configuration lateral side the drag still 24% higher. Consequently the new 3-D configuration drag was 13% higher than the 3-D clean configuration drag. The vortex in the upside inlet shown in Figure 14 shows that the system could be further improved for this fan condition as the suction coefficient is still not

enough to achieve complete attachment of the boundary layer and maximum drag reduction [1]. Even so, the fan thrust, which is ten times higher than the body drag, contributes positively the total forward force.

The 3-D results for other operational fan conditions are shown in Figure 20. Although the new wheel fairing displays a higher drag for the fan off, increasing the suction coefficient reduces the drag to a point where the aerodynamic force overpowers the fairing drag and creates “pressure thrust” [2].

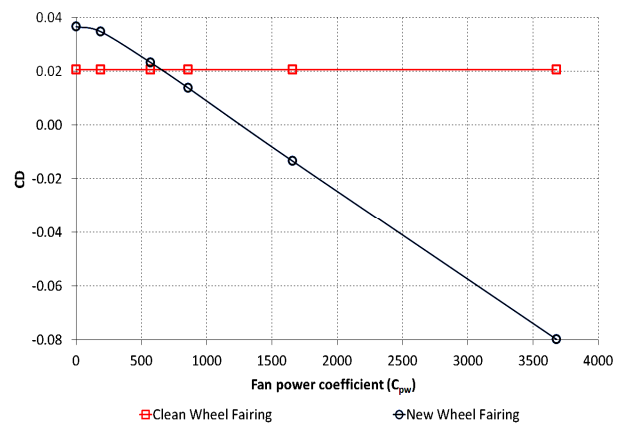


Figure 20 – Drag force as function of fan power.

4. Conclusion and Future Work

The proposed methodology allows the achievement of engineering knowledge regarding the system space design. The main parameters and their influence on the system performance were identified and directives to future design optimization were discovered. It is important to remark the importance of the design space exploration before a design optimization effort, because greater knowledge regarding the system allows better engineering design decisions, such as choosing more intelligent parameters range which allows one to run a high fidelity design optimization.

The fan inlet gap was identified as a key parameter that directly affects the system performance and, contrary to preconceptions regarding the Goldschmied-Skaleski propulsion concept, increasing the lift on the shroud airfoil does not necessarily produce the best results.

The 3-D model of the new wheel fairing configuration presented 13% more drag than the

clean configuration in the fan operational point of 4,424 Pa. But the net force in the x axis becomes more negative once a fan provides thrust and boundary layer suction. Furthermore, for high power conditions, the system presented an extreme drag reduction; to the point where the aerodynamic force creates “pressure thrust”. This shows that fan condition is a constraint to the system performance, once that it is not physically possible to obtain a high power fan unit for the specified dimensions. Other constraining factor are the air inlet Mach number, because high power implies in high air mass flow through the fan; the airspeed over the shroud airfoil could reach conditions where the wave drag becomes a factor, and even a shockwave might develop in the air inlet.

The next steps are to take a high fidelity design optimization using the engineering knowledge obtained and to build a real electric ducted fan which will be tested in wind tunnel. Only when the new wheel fairing is tested in flight it will be possible to measure the advantages of this system design, because the drag reduction is a function of the fan thrust that depends on dynamic conditions provided by the airplane performance. Considering it succeeds, the present concept could be studied to transonic aircrafts and nacelles applications, even other transport vehicles such as cars and submarines.

References

- [1] Cecil Skaleski, "Analysis of Goldshimied's Propulsive Concept for the Design of Bodies with Integrated Propulsion(in Portuguese the original title is: Análise do Conceito Propulsor de Goldshimied para o Projeto de Corpos com Propulsão Integrada)," Instituto Tecnológico de Aeronáutica, São José dos Campos, SP, [Masters Thesis] 2014.
- [2] Fabio Goldschmied, "Fuselage Self-Propulsion by Static-Pressure Thrust: Wind-Tunnel Verification," in *AIAA/AHS/ASEE Aircraft Design, Systems and Operations Meeting*, St. Louis, MO, 1987. AIAA-87-2935.
- [3] Joshua Roepke, "An Investigation of a Goldschmied Propulsor," California Polytechnic State University, San Luis Obispo, CA, [Masters Thesis] 2012.
- [4] Cory Seubert, "Analysis of a Goldschmied Propulsor Using Computational Fluid Dynamics Referencing California Polytechnic's Goldschmied Propulsor Testing," California Polytechnic State University, San Luis Obispo, CA, [Masters Thesis] 2012.
- [5] Nicole Thomason, "Experimental investigation of suction slot geometry on a Goldschmied propulsor," California Polytechnic State University, San Luis Obispo, CA, [Masters Thesis] 2012.
- [6] Sighard F. Hoerner, *Fluid Dynamic Drag: practical information on aerodynamic drag and Hydrodynamic resistance*. Brick, NJ: Hoerner Fluid Dynamics, 1965.
- [7] Metacomp Technologies, Inc. CFD++. [Program].
- [8] Dassault Systemes. CATIA V5. [Program].
- [9] ANSYS. ICEM CFD. [Program].
- [10] Douglas C. Montgomery, *Design and Analysis of Experiments*, 5th ed. New York: Wiley, 2001.

Contact Author Email Address

cecil.skaleski@embraer.com.br

Copyright Statement

The authors confirm that they, and/or their company or organization, hold copyright on all of the original material included in this paper. The authors also confirm that they have obtained permission, from the copyright holder of any third party material included in this paper, to publish it as part of their paper. The authors confirm that they give permission, or have obtained permission from the copyright holder of this paper, for the publication and distribution of this paper as part of the ICAS 2014 proceedings or as individual off-prints from the proceedings.